Journal of Organometallic Chemistry 695 (2010) 1323–1327

Contents lists available at ScienceDirect

Journal of Organometallic Chemistry

journal homepage: www.elsevier.com/locate/jorganchem

Synthesis and characterization of ferrocenyl-acridine dyads and their multiresponse to proton and metal cations

Qian-Yong Cao *, Xin Lu, Zhi-Hua Li, Li Zhou, Zhen-Yu Yang, Jiang-Hua Liu

Department of Chemistry, Nanchang University, 999 Xuefu Road, Nanchang 330031, China

ARTICLE INFO

Article history:
Received 5 December 2009
Received in revised form 10 February 2010
Accepted 12 February 2010
Available online 17 February 2010

Keywords:
Ferrocene
Acridine
Prontonation
Metal cations
Electrochemistry
Optical spectroscopy

ABSTRACT

Two new π-conjugated linked ferrocenyl-acridine dyads, (9-ethynylferrocenyl)acridine (**3a**) and (1-(ferrocenylethynyl)-4-ethynylbenzenyl)-acridine (**3b**), have been synthesized and investigated. UV–Vis spectroscopic and electrochemical studies reveal that **3a** offers stronger electronic communication between terminal subunits than the extended system **3b**, as shown by a stronger and lower-energy metal-to-ligand charge transfer (MLCT) transition and a more positive redox potential. Both of **3a** and **3b** show multiresponse to protons and selected metal ions (M = Zn^{2+}, Pb^{2+}, Hg^{2+}, Fe^{3+}, Cr^{3+}), with a MLCT transition shift to the lower-energy, a redox potential shift to anode, and a luminescence increasing.

1. Introduction

Photoactive donor-conjugated link-acceptor dyads have attracted significant attention due to their potential applications in biological systems [1,2], solar cells [3,4], and nonlinear optical (NLO) devices [5–7]. Ferrocenes are good donor moieties for their well-behaved redox chemistry, chemical robustness and synthetic versatility [8]. In the past decade, many novel Fc-donor organic-acceptor dyads have been synthesized and characterized [9–15]. Some of these conjugated systems offer strong electronic communication between terminal subunits, and display enhanced second-order NLO properties [11–14]. Although these studies have covered a large number of organic acceptors, as well as the use of different conjugated units, there is still much scope for the development of new dyads. Moreover, Fc-donor organic-acceptor dyads incorporating organic fluorescent moieties are really rare [15,16]. Although ferrocenyl derivatives are well known as efficient luminescence quenchers, it has emerged that ferrocenyl groups may be advantageously used as redox centers in multiresponsive, photo- and electrochemically active assemblies [8,17–20].

Acridines are good candidates as components of fluorescent dyads because they often exhibit strong solvatochromatic fluorescence [21–23]. Owing to the presence of a nitrogen atom in the rings, these compounds are weak organic bases capable of adding a proton in acidic media, or coordinating with metal ions. Their electronic spectra may change accordingly [23–26]. Finally, previous studies indicate that the presence of hetero-aromatics in conjugated Fc-donor organic-acceptor dyads is highly beneficial for the observation of large NLO properties [14]. Recently, Robinson et al. have reported the neutral and oxidation state electronic spectra of 2- or 2,7-position ethynylferrocene substituted acridine dyads [15c]. However, their effects on proton and metal cations have not been discussed. Herein, we report two new ferrocenyl derivatives of acridine on the 9-position with ethynyl (**3a**) or phenyl–ethynyl (**3b**) spacer. Their electronic spectra, electrochemical properties and effects on proton and metal cations are also discussed.

2. Results and discussion

2.1. Synthesis

The new ferrocenyl-acridine dyads (**3a** and **3b**) were prepared by Sonogashira coupling of ethynylferrocene (**1a**) or 1-(ferrocenylethynyl)-4-ethynylbenzene (**1b**) with 9-chloroacridine (**2**) in THF/Et_3N (1:1,V/V) solution (Scheme 1). After appropriate workup, **3a** and **3b** were obtained as orange, air-stable solids in yields of 68% and 20%, respectively. Both compounds can be dissolved in many organic solvents, such as petroleum ether, toluene, diethyl ether and dichloromethane. Their structures were characterized by ^1H NMR and IR spectroscopy.

2.2. Spectroscopic and redox properties

Both **3a** and **3b** show strong structured absorption bands between 350 and 450 nm (Fig. 1 and Table 1), with **3a** peaking at 367

* Corresponding author. Tel.: +86 791 3969252; fax: +86 791 3969386.
E-mail address: cqyong@ncu.edu.cn (Q.-Y. Cao).

0022-328X/$ - see front matter © 2010 Elsevier B.V. All rights reserved.
doi:10.1016/j.jorganchem.2010.02.013

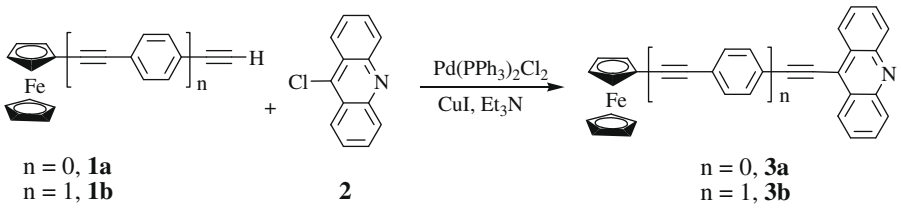

Scheme 1. Synthetic approach for compound **3a** and **3b**.

and 393 nm, and **3b** at 371, 406 and 426 nm, respectively. These bands can be ascribed to the acridine chromophore π–π* or n–π* transition, which are in agreement with the reported data of ethyne-based acridine derivatives [27]. The red shift bands of the acridine bands of **3b** compared to those of **3a** can be attributed to the increased conjugation effect, which most likely lowers the energy of the π* orbital. In addition, compound **3a** shows a moderate and broad band between 450 and 600 nm with λ_{max} at 498 nm ($\varepsilon = 1.1 \times 10^3$ L M^{-1} cm^{-1}), which can be ascribed to the metal-to-ligand charge transfer (MLCT) from Fe(II) d-orbitals to π-orbitals of conjugated acridine moiety [10]. The MLCT transition for **3b** is not resolved from the tail of the acridine absorption, but might be expected between 450 and 550 nm. The equivalent absorption for ferrocenylethynylbenzene occurs at 446 nm ($\varepsilon = 0.5 \times 10^3$ L mol^{-1} cm^{-1}) [15a]. Importantly there are also likely to be significant self absorption effects between chromophore and lumophore. The results however suggest the degree of communication between the Fc-donor and acridine acceptor for **3a** is attenuated by the interpolated spacer for **3b**.

Both the acridine chromophore π–π* transition and the MLCT transition of the two dyads show positive solvatochromism with increasing solvent polarity (Fig. 1). For example, the MLCT transition of **3a** bathochromically shifts from 460 nm in hexane to 501 nm in EtOH solution, at the same time, the π–π* transition shifts from 385 to 393 nm. When **3a** is investigated in dimethyl sulfoxide, a drastic change in the spectra is noticed that the red shift of MLCT band to 618 nm with large extinction coefficient ($\varepsilon = 3.7 \times 10^3$ L M^{-1} cm^{-1}). Similar results were also reported by Lin et al. in Fc-donor dicyanovinyl substituted thiophene and furan acceptor dyads [28].

Though the ferrocenyl is well known as an efficient luminescence quencher, both **3a** and **3b** retain their parent acridine moiety vibrational fine structure emission in CH_3CN solution with maximal wavelengths at 436 and 446 nm, respectively (Fig. 2 and Table 1). The small Stokes shifts for both compounds (38 nm for **3a** and 42 nm for **3b**) indicate that they are essentially "acridine" emission [27].

Table 1
UV–Vis absorption, emission and electrochemical data of the studied dyads.

Dyads	λ_{abs} (ε)[a]	λ_{em}[b]	$E_{1/2}$[c]	ΔE_p[d]
3a	367(4.5), 393(4.0), 498(1.1)	436	0.245	
3aH$^+$	368(6.9), 458(4.5), 665(1.8)	506	0.365	0.115
3a–Fe^{3+}	367(8.7), 458(4.7), 665(1.9)	507	–	0.095
3a–Pb^{2+}	367(7.0), 456(4.1), 668(1.8)	510	–	0.075
3a–Zn^{2+}	367(8.1), 456(4.4), 665(1.9)	463	–	0.07
3a–Cr^{3+}	367(7.8), 458(2.6), 669(2.1)	509	–	0.09
3a–Hg^{2+}	367(9.0), 457(5.5), 669(2.3)	510	–	0.085
3b	371(6.6), 406(8.7), 426(7.6)	446	0.21	
3bH$^+$	371(8.5), 406(4.9), 466(5.3)	432, 520	0.23	0.03
3b–Fe^{3+}	371(8.4), 406(7.2), 465(8.3)	524	–	0.015
3b–Pb^{2+}	371(7.6), 406 (7.4), 463(4.3)	508	–	0.01
3b–Zn^{2+}	371(5.9), 406 (7.0), 464(2.3)	442, 458	–	0.01
3b–Cr^{3+}	371(8.5), 405(5.5), 466(7.6)	505	–	0.015
3b–Hg^{2+}	371(7.0), 406 (6.3), 465(4.6)	522	–	0.01

All data were obtained in acetonitrile at 20 °C.
[a] λ_{max}/nm, ε/10^3 L mol^{-1} cm^{-1}, high-energy bands > 300 nm not given.
[b] λ_{max}/nm, λ_{ex} at 360 nm (**3a**) and 370 nm (**3b**).
[c] $E_{1/2}$/V, cyclic voltammetry (CV), a Pt disk working electrode, *n*-Bu_4NPF_6 as supporting electrolyte scanned at 100 mV s^{-1}.
[d] The value of anodical shift in presence of proton or metal ions by differential pulse voltammetry (DPV).

Cyclic voltammograms (CVs) of **3a** and **3b** were recorded under dinitrogen in CH_3CN/0.1 M *n*-Bu_4NPF_6 solution. Both complexes show one reversible ferrocene-centered redox wave with an $E_{1/2}$ value of 0.245 V for **3a** and 0.210 V for **3b**, respectively (Fig. 3 and Table 1). The observation of the $E_{1/2}$ value of **3b** at more positive potential than **3b** confirms the weaker interaction between ferrocene donor and acridine acceptor in the benzene spacer compound [9].

2.3. Effect of proton acid

The UV–Vis spectra of **3a** and **3b** upon addition of increasing amounts of HBF_4 in acetonitrile solution are shown in Fig. 4. Upon

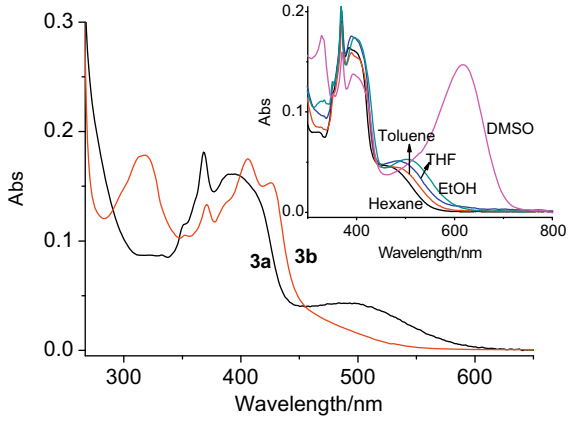

Fig. 1. UV–Vis spectra of compound **3a** (40 μM) and **3b** (20 μM) in CH_3CN solution. Inset: solvent effect of compound **3a**.

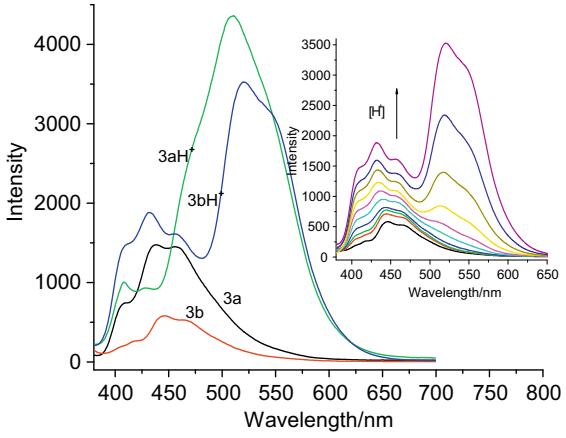

Fig. 2. Fluorescent spectra of compound **3a** (40 μM), **3b** (20 μM), **3a**·H$^+$ and **3b**·H$^+$ in CH_3CN solution. Inset: fluorescent spectra of compound **3b** (20 μM, excitation at 370 nm) in presence of HBF_4·Et_2O (0–5 equiv.).

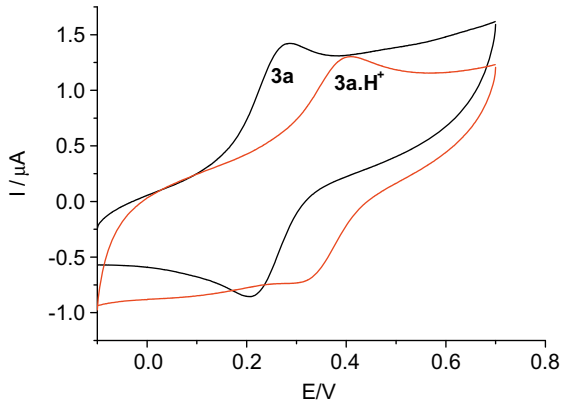

Fig. 3. Cyclic voltammetrys of **3a** (400 μM) in the absence (black) and presence (red) of $HBF_4{\cdot}Et_2O$ (5 equiv.) in CH_3CN solution using $[Bu_4N]PF_6$ (0.1 M) as the supporting electrolyte with a scan rate of 100 mV s^{-1}. (For interpretation of the references to colour in this figure legend, the reader is referred to the web version of this article.)

addition of $HBF_4{\cdot}Et_2O$ to the acetonitrile solution of **3a**, two bands centered at 458 and 665 nm are formed and developed, with the band centered at 498 nm decreasing and vanishing. The solution color changed from yellow to green. Red shift of the absorption spectra and the presence of clear isosbestics points at 296, 382 and 421 nm together indicate a new species corresponding to the protonation of nitrogen on the acridine fluorophore. The process is reversible, with aqueous NaOH caused complete regeneration of the original spectrum of the dyad. This demonstrates that the HBF_4 initiated spectra changes are due to reversible acid–base equilibria. The band centered at 458 nm can be attributed to protonation the acridine moiety, which is similar to the spectra of some reported protonation acridines [24–26]. While band centered at 665 nm assigned to MLCT transition. The MLCT band with a remarkable bathochromic shift ($\Delta\lambda$ = 167 nm) indicates that the protonated **3a**·$\mathbf{H^+}$ is an efficient electron acceptor, which makes the charge transfer easier. The absorption changes of **3b** upon gradual titration with HBF_4 are different from those of **3a**. As the HBF_4 concentration increases, only one new broad band which attributed to protonation the acridine moiety at 466 nm is gradually observed, with peak at 371 nm increasing, and peaks at 406 and 426 nm decreasing. The three well-defined isosbestic points at 326, 385 and 435 nm indicate that a neat interconversion between the neutral and protonal species. Though the absorption spectrum of **3b** solution has altered, its color (yellow) shows no obviously change.

The emission spectra of both **3a** and **3b** in protonal forms are also different from those in neutral forms (Fig. 2 and Table 1). For **3a**, the intensity of band centered at 436 nm decreases with increasing HBF_4 concentration, which is accompanied by a new band located at 506 nm appearing gradually. The integrated emission intensity of the protonal species is enormously increases. Similar results are also reported for related acridine compounds [25,26]. The emission spectra of **3b** also show enhanced fluorescence effect after protonation. With increasing HBF_4 concentration, the intensity of the band centered at 446 nm increases and blue shifts to 432 nm. In addition, a new band at 520 nm is observed and increased accordingly.

The electrochemical behavior of both compounds in the presence of HBF_4 was investigated by cyclic voltammogram (CV) and differential pulse voltammetry (DPV). With the addition of excess HBF_4 to the solution of both compounds in CH_3CN, the redox potential of the ferrocene nucleus shifts to anode (Fig. 3 and Table 1). The protonation-induced redox potential shift of **3a** ($\Delta E_{1/2}$ = 120 mV and ΔE_p = 115 mV) is larger than that of **3b** ($\Delta E_{1/2}$ = 30 mV and ΔE_p = 30 mV), which indicates stronger communication between Fc and protonated acridine moiety in **3a** than that in the extended D–A system **3b**.

2.4. Coordination on cations

The metal-coordination properties of both compounds were also investigated by UV–Vis spectra, emission spectra and electrochemical properties. Perchlorates of representative alkali ions (Li^+, Na^+), alkaline earth ions (Mg^{2+}, Ba^{2+}), and transition metal ions (Ag^+, Ni^{2+}, Co^{2+}, Cd^{2+}, Zn^{2+}, Pb^{2+}, Hg^{2+}, Fe^{3+}, Cr^{3+}) were used. The absorption titration experiments show that addition of Zn^{2+}, Pb^{2+}, Hg^{2+}, Fe^{3+} and Cr^{3+} to **3a** and **3b** give rise to similar changes in the UV–Vis spectra, but other ions show no obvious effects (Fig. 5 and Table 1). This is reasonable since the acridine can only coordinate some metal ions [23]. We take Pb^{2+} for an example to explain the detailed absorption changes by adding these metal ions. Fig. 6 shows spectrophotometric changes upon titrating a fixed concentration of **3a** (40 μM) with incremental addition of $Pb(ClO_4)_2$ in acetonitrile. For **3a**, the new band based on acridine moiety coordinate the metal ion at 456 nm ($\varepsilon = 4.1 \times 10^3$ L M^{-1} cm^{-1}) is observed, and a red shift of the MLCT transition from 500 to 668 nm ($\varepsilon = 1.8 \times 10^3$ L M^{-1} cm^{-1}) is found. The red shift is in accord with the coordination induced enhance-

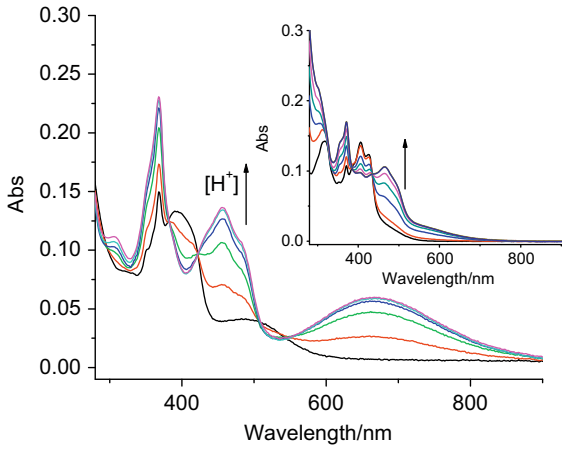

Fig. 4. UV–Vis spectra of compound **3a** (40 μM) and **3b** (inset figure, 20 μM) on titration with $HBF_4{\cdot}Et_2O$ (0–5.0 equiv.) in CH_3CN solution.

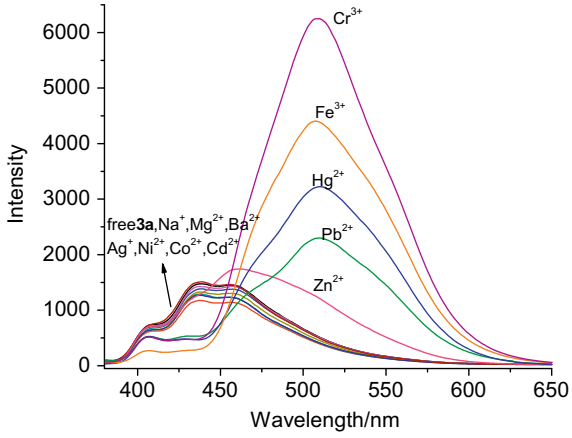

Fig. 5. Fluorescent changes of compound **3a** (40 μM) in the absence and presence of excess amount of selected metal perchlorates in CH_3CN solution (excitation at 360 nm).

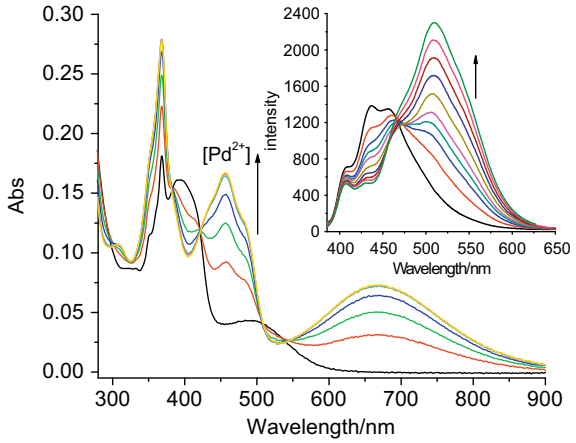

Fig. 6. UV–Vis spectra and Fluorescent (inset: excitation at 360 nm) changes of compound **3a** (40 μM) on titration with Pb^{2+} cations (0–20.0 equiv.) in CH_3CN solution.

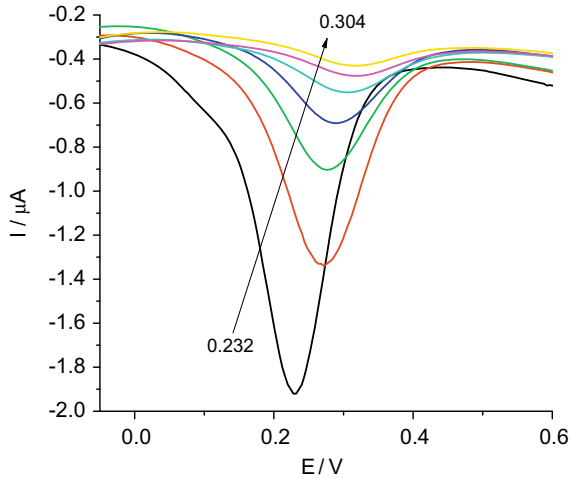

Fig. 7. DPV (50 ms pulse width) of free **3a** (black) (400 μM) on titration with Zn^{2+} cation (0–20.0 equiv.) in CH_3CN solution showing the changes of peak potentials.

ment of the MLCT course from the donor ferrocenyl groups to the metal-bound acridine acceptor, and was reported on related ferrocene-based complexes [29,30]. When **3b** coordinates to Pb^{2+}, a new band at 463 nm is observed, with the weak energy transition tails beyond 700 nm, which is similar to that of protonation **3b**.

The emission titration experiments show that addition of metal ions mentioned above to **3a** or **3b** results in a selected coordination enhanced fluorescence effect (Fig. 5 and Table 1). For **3a**, by adding Pb^{2+}, Hg^{2+}, Fe^{3+} or Cr^{3+} ions, the similar coordination enhanced fluorescence effect is observed, with decreasing of emission at 436 nm, and increasing of a new band at 507–510 nm. However, it shows a weak fluorescence enhancement changes by adding Zn^{2+}. After adding excess amount of Zn^{2+} to **3a**, the emission at 436 nm still sustains, and a new band at 463 nm appears. For **3b**, coordination enhanced fluorescence effect can only be observed by adding Hg^{2+}, Fe^{3+} or Cr^{3+}, with the λ_{max} red shift to 522, 524 and 505 nm, respectively. However, Zn^{2+} and Pb^{2+} lead to weak quenching effect.

The electrochemical behavior of both compounds was also investigated after coordinating metal ions by DPV. For **3a**, a strong anodical shift of the oxidation peak is observed by stepwise addition of Zn^{2+}, Pb^{2+}, Hg^{2+}, Fe^{3+} and Cr^{3+} ions to the electrochemical solution, with anodical shifts of 70, 75, 85, 95 and 90 mV, respectively. However, **3b** shows only weak anodical shift range from 10 mV (Zn^{2+} and Pb^{2+}) to 15 mV (Fe^{3+}) upon adding these metal ions (Fig. 7 and Table 1). Fig. 7 shows the detailed DPV process upon addition of Zn^{2+} ion to **3a** solution (400 μM) for an example. On stepwise addition of Zn^{2+} ion to an electrochemical solution of **3a**, a strong anodical shift of the oxidation peak from 0.230 to 0.300 V (ΔE_p = 70 mV) is observed. The value of anodical shift in presence of these metal ions is comparable to that of upon protonation, which indicates that coordinating metal ions increases the acceptor electron-withdrawing ability. The anodical shift of the oxidation peak of **3a** after coordinating metal ions is larger than that of **3b**, indicating strong communication between the Fc-donor and acridine acceptor in **3a** than that in **3b**.

3. Conclusion

In summary, we have successfully prepared two new π-conjugated spacer linked ferrocenyl-acridine dyads **3a** and **3b**. Electronic spectral and electrochemical studies show that the simple ethynyl spacer connected **3a** has stronger communication between the ferrocene donor and acridine acceptor, which is enhanced after protonation or coordination selected metal ions. Multiresponse to proton and selected metal ions and strong charge transfer effect of both compounds make them prospective candidates for chemical sensors or nonlinear optical (NLO) materials.

4. Experimental

4.1. Materials and methods

Solvents were dried using the standard procedures. Ethynylferrocene (**1a**) [31] 1-(ferrocenylethynyl)-4-ethynylbenzene (**1b**) [32] and 9-chloroacridine (**2**) [33] were prepared by the literature procedures. The commercial reagents were used without further purification. All metal ions of perchlorate salts were purchased from the Alfa Aesar Chemical Company. Their stock solutions were prepared in acetonitrile (*Warning! Perchlorate salts are hazardous because of the possibility of explosion!*)

^1H NMR spectra were recorded with a Varian spectrometer at 400 MHz. Chemical shifts, given in ppm. Electron absorption spectra were recorded on a Shimadzu UV-2300 spectrometer. Luminescence spectra were measured on a Hitachi F-4500 fluorescence spectrophotometer. Electrochemical measurements were performed with CHI 610C. All electrochemical measurements were carried out in a one-compartment cell under a nitrogen atmosphere at 25 °C, equipped with a Pt disk working electrode, a platinum wire counter electrode, and Ag/Ag^+ (0.1 M) reference electrode. All potentials are quoted relative to Ag/Ag^+, with the parent ferrocene $E_{1/2}$ = 0.035 V. The supporting electrolyte was a 0.10 M acetonitrile solution of tetrabutylammonium hexafluorophosphate (n-Bu_4NPF_6). The scan rate was 100 mV s^{-1}. Differential pulse voltammetry (DPV) measurements were also carried out using a CHI 610C with a 50 ms pulse width.

For proton and metal cation detection experiments, concentrated acetonitrile solutions of HBF_4 and tetrabutylammonium salts of the respective anions were titrated into **3a** (40 μM) or **3b** (20 μM) in the same solvent, keeping the total volume of the mixture constant.

4.2. Synthesis of *3a*

Under nitrogen atmosphere, a solution containing ethynylferrocene (**1a**) (212 mg, 1 mmol), 9-chloroacridine (**2**) (213 mg, 1 mmol), $PdCl_2(PPh_3)_2Cl_2$ (21 mg, 0.03 mmol) and CuI (6 mg, 0.03 mmol) in triethylamine/tetrahydrofuran (40 mL, V/V, 1/1)

was heated under refluxing for 15 h. The reaction mixture was filtered and the filtrate was evaporated under reduced pressure. Yellow solid **3a** was obtained by column chromatogramph on silica gel with CH_2Cl_2/petroleum ether (V/V, 2/1) as eluent. Yield: 263 mg (68%). ^{1}H NMR ($CDCl_3$, δ): 4.33 (s, 5H, C_5H_5), 4.43 (s, 2H, C_5H_4), 4.76 (s, 2H, C_5H_4), 7.65 (t, J = 7.6 Hz, 2H, acridine H), 7.81 (t, J = 7.6 Hz, 2H, acridine H), 8.24 (d, J = 8.7 Hz, 2H, acridine H), 8.52 (d, J = 8.5 Hz, 2H, acridine H). IR (KBr, cm^{-1}): $\nu_{(C\equiv C)}$ 2208. Anal. Calc. for $C_{25}H_{17}FeN$ (387.26): C, 77.54; H, 4.42; N, 3.62. Found: C, 77.66; H, 4.50; N, 3.51%.

4.3. Synthesis of *3b*

Compound **3b** was prepared as yellow solid in a similar way to **3a** except that 1-(ferrocenylethynyl)-4-ethynylbenzene (**1b**) was used in place of ethynylferrocene (**1a**). Yield: 20%. ^{1}H NMR ($CDCl_3$, δ): 4.28 (s, 5H, C_5H_5), 4.30 (s, 2H, C_5H_4), 4.55(s, 2H, C_5H_4), 7.59 (d, J = 8.0 Hz, 2H, Ar–H),7.66 (t, J = 7.6 Hz, 2H, acridine H), 7.75 (d, J = 8.0 Hz, 2H, Ar–H), 7.83 (t, J = 7.6 Hz, 2H, acridine H), 8.26 (d, J = 8.6 Hz, 2H, acridine H), 8.58 (d, J = 8.5 Hz, 2H, acridine H). IR (KBr, cm^{-1}): $\nu_{(C\equiv C)}$ 2215, 2241. Anal. Calc. for $C_{33}H_{21}FeN$ (487.39): C, 81.32; H, 4.34; N, 2.87. Found: C, 81.19; H, 4.51; N, 2.69%.

Acknowledgments

This work was supported by NSFC (20963007 and 20703023), the Bureau of Education of Jiangxi Province (GJJ09074) and the program for innovative research team of Nanchang University. We are also grateful to financial support from Nanchang University for young teachers.

References

[1] D. Gust, T.A. Moore, A.L. Moore, Acc. Chem. Res. 26 (1993) 198–205.
[2] D. Gust, T.A. Moore, A.L. Moore, Acc. Chem. Res. 34 (2001) 40–48.
[3] M. Gratzel, Inorg. Chem. 44 (2005) 6841–6851.
[4] J.P. Sauvage, J.P. Collin, J.C. Chambron, S. Guillerez, C. Coudret, V. Balzani, F. Barigelletti, L.D. Cola, L. Flamigni, Chem. Rev. 94 (1994) 993–1019.
[5] S.D. Bella, Chem. Soc. Rev. 30 (2001) 355–366.
[6] D.R. Kanis, M.A. Ratner, T.J. Marks, Chem. Rev. 94 (1994) 195–242.
[7] F. Tessore, D. Roberto, R. Ugo, M. Pizzotti, S. Quici, M. Cavazzini, S. Bruni, F.D. Angelis, Inorg. Chem. 44 (2005) 8967–8978.
[8] S. Fery-Forgues, B. Delavaux-Nicot, J. Photochem. Photobiol. A: Chem. 132 (2000) 137–159.
[9] (a) P. Debroy, S. Roy, Coord. Chem. Rev. 251 (2007) 203–221;
(b) E. Peris, Coord. Chem. Rev. 248 (2004) 279–297.
[10] O.N. Chupakhin, I.A. Utepova, I.S. Kovalev, V.L. Rusinov, Z.A. Starikova, Eur. J. Org. Chem. (2007) 857–862.
[11] S. Barlow, H.E. Bunting, C. Ringham, J.C. Green, G.U. Bublitz, S.G. Boxer, J.W. Perry, S.R. Marder, J. Am. Chem. Soc. 121 (1999) 3715–3723.
[12] S. Barlow, S.R. Marder, Chem. Commun. (2000) 1555–1562.
[13] Y. Liao, B.E. Eichinger, P.J. Reid, A.K.-Y. Jen, L.R. Dalton, B.H. Robinson, J. Am. Chem. Soc. 127 (2005) 2758–2766.
[14] (a) J.A. Mata, E. Peris, I. Asselberghs, R. Van Boxel, A. Persoons, New J. Chem. 25 (2001) 1043–1046;
(b) Y. Liao, B.E. Eichinger, K.A. Firestone, J. Luo, W. Kaminsky, J.B. Benedict, P.J.J.A. Mata, S. Uriel, R. Llusar, E. Peris, Organometallics 19 (2000) 3797–3802.
[15] (a) L. Cuffe, R.D.A. Hudson, J.F. Gallagher, S. Jennings, C.J. McAdam, R.B.T. Connelly, A.R. Manning, B.H. Robinson, J. Simpson, Organometallics 24 (2005) 2051–2060;
(b) C.J. McAdam, J.L. Morgan, B.H. Robinson, J. Simpson, P.H. Rieger, A.L. Rieger, Organometallics 22 (2003) 5126–5136;
(c) E.M. McGale, B.H. Robinson, J. Simpson, Organometallics 22 (2003) 931–939.
[16] I.R. Butler, A.G. Callabero, G.A. Kelly, J.R. Amey, T. Kraemer, D.A. Thomas, M.E. Light, T. Gelbrich, S.J. Coles, Tetrahedron Lett. 45 (2004) 467–472.
[17] (a) P.D. Beer, A.R. Graydon, L.R. Sutton, Polyhedron 15 (1996) 2457–2461;
(b) P.D. Beer, F. Szemes, V. Balzani, C.M. Sala, M.G.B. Drew, S.W. Dent, M. Maestri, J. Am. Chem. Soc. 119 (1997) 11864–11875.
[18] (a) B. Delavaux-Nicot, J. Maynadie, D. Lavabre, S. Fery-Forgues, Inorg. Chem. 45 (2006) 5691–5702;
(b) B. Delavaux-Nicot, J. Maynadie, D. Lavabre, S. Fery-Forgues, J. Organomet. Chem. 692 (2007) 3351–3362.
[19] (a) K.W. Huang, H. Yang, Z.G. Zhou, F.Y. Li, X. Gao, T. Yi, C.H. Huang, Org. Lett. 10 (2008) 2557–2560;
(b) H. Yang, Z.G. Zhou, K.W. Huang, F.Y. Li, T. Yi, C.H. Huang, Org. Lett. 9 (2007) 4729–4732.
[20] A. Caballero, R. Martínez, V. Lloveras, I. Ratera, J. Vidal-Gancedo, K. Wurst, A. Tarraga, P. Molina, J. Veciana, J. Am. Chem. Soc. 127 (2005) 15666–15667.
[21] J. Herbich, A. Kapturkiewicz, J. Am. Chem. Soc. 120 (1998) 1014–1029.
[22] O. Rubio-Pons, L. Serrano-Andres, M. Merchan, J. Phys. Chem. A 105 (2001) 9664–9673.
[23] M.S. Park, K.M.K. Swamy, Y.J. Lee, H.N. Lee, Y.J. Jang, Y. Hyun Moon, J. Yoon, Tetrahedron Lett. 47 (2006) 8129–8132.
[24] E.T. Ryan, T. Xiang, K.P. Johnston, M.A. Fox, J. Phys. Chem. A 101 (1997) 1827–1835.
[25] T. Pedzinski, B. Marciniak, G.L. Hug, J. Photochem. Photobiol. A: Chem. 150 (2002) 21–30.
[26] L.G. Samsonova, N.I. Selivanov, T.N. Kopylova, V.Y. Artyukhov, G.V. Maier, V.G. Plotnikov, V.A. Sazhnikov, A.A. Khlebunov, M.V. Alfimov, High Energy Chem. 43 (2009) 105–115.
[27] A. Elangovan, H. Chiu, S. Yang, T. Ho, Org. Biomol. Chem. 2 (2004) 3113–3118.
[28] K.R.J. Thomas, J.T. Lin, Y.S. Wen, J. Organomet. Chem. 575 (1999) 301–309.
[29] A. Caballero, V. Lloveras, D. Curiel, A. Tárraga, A. Espinosa, R. García, J. Vidal-Gancedo, C. Rovira, K. Wurst, P. Molina, J. Veciana, Inorg. Chem. 46 (2007) 825–838.
[30] T.J.J. Müller, A. Netz, M. Ansorge, K. Meerholz, Organometallics 18 (1999) 5066–5074.
[31] J. Polin, H. Schottenberger, Org. Synth. Coll. Vol. 9 (1998) 411–415.
[32] R.P. Hsung, C.E.D. Chidsey, L.R. Sita, Organometallics 14 (1995) 4808–4815.
[33] A. Albert, B. Ritchie, Org. Synth. Coll. Vol. 3 (1955) 53–56.